RSC Advances

Electronic Supplementary Information

Tuning SEI formation on nanoporous carbon-titania composite sodium ion batteries anodes and performance with subtle processing changes

Received 00th January 20xx,
Accepted 00th January 20xx

DOI: 10.1039/x0xx00000x

www.rsc.org/

Jeongwoo Lee[a], Yu-Ming Chen[b], Yu Zhu[b], and Bryan D. Vogt[a,*]

[a] Department of Polymer Engineering, University of Akron, Akron, OH 44325.
[b] Department of Polymer Science, University of Akron, Akron, OH 44325.
* To whom correspondence should be addressed: vogt@uakron.edu

Figure S1 illustrates the morphology of the porous carbon/TiO_2 composite fabricated using 0.35 g PHEMA/0.3 g FA/0.3 g TiO_2 as a function of molecular weight of PHEMA (20K, 300K, and 1000K). The pores of the carbon/TiO_2 composite are significantly larger for the composite produced using 20K PHEMA (Figure S1A) than the carbon/TiO_2 composites from 300K (Figure S1B) and 1000K PHEMA (Figure S1C). The morphology of porous carbon/TiO_2 composites pyrolyzed from PHEMA/FA/TiO_2 appears to be controlled by the mobility of the precursor suspension that decreases as the molecular weight of PHEMA increases. Additionally, agglomeration of the TiO_2 nanoparticles increases as the molecular weight of PHEMA increases.

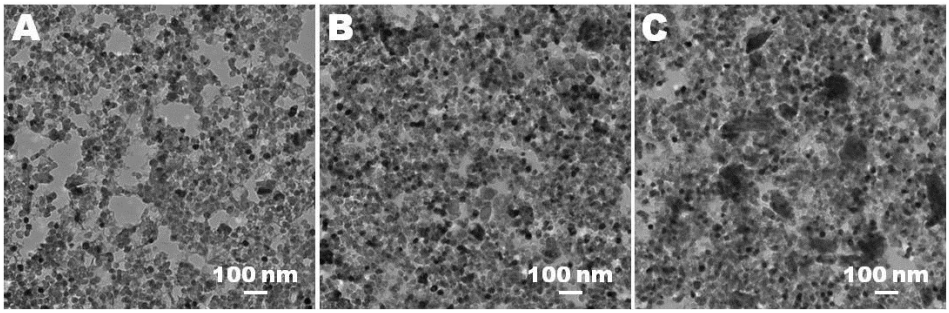

Figure S1. TEM micrographs of porous carbon/TiO_2 composites fabricated with (A) 20K, (B) 300K, and (C) 1000K PHEMA using 0.35 g PHEMA /0.3 g FA/0.3 g TiO_2 for the precursor.

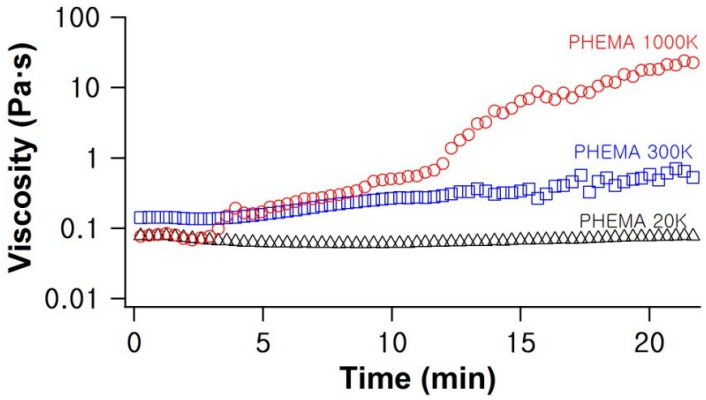

Figure S2. Viscosity variation of FA/PHEMA solutions with different molecular weight of PHEMA during FA polymerization.

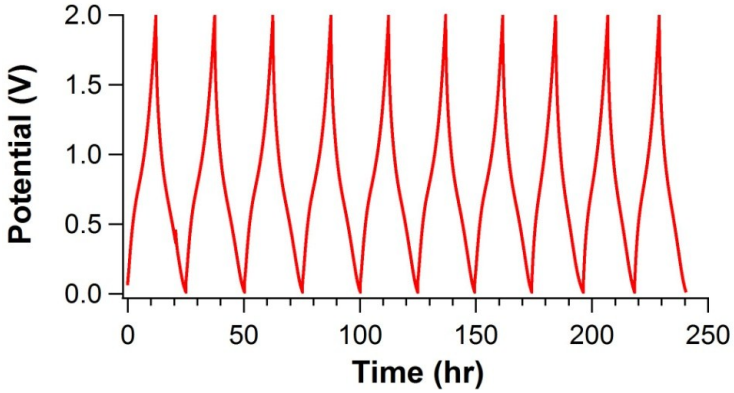

Figure S3.Galvanostatic charge/discharge behavior of carbon/TiO_2 composites from 20K pf PHEMA in a potential range of 0.01–2.0 V at a current density of 10 mA/g.

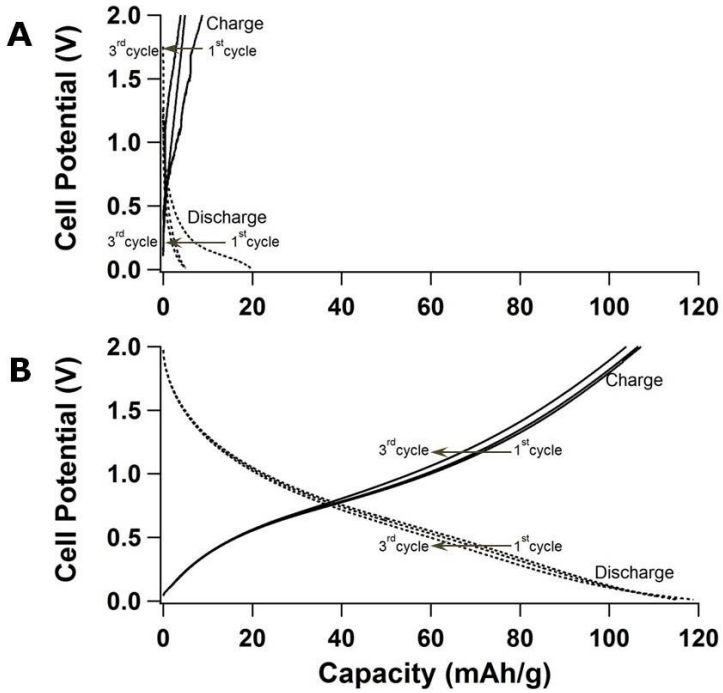

Figure S4. Galvanostatic charge/discharge behavior of (A) TiO_2 and (B) carbon/TiO_2 composites from 20K of PHEMA and 0.3 g of FA in a potential range of 0.01–2.0 V at a current density of 10 mA/g.

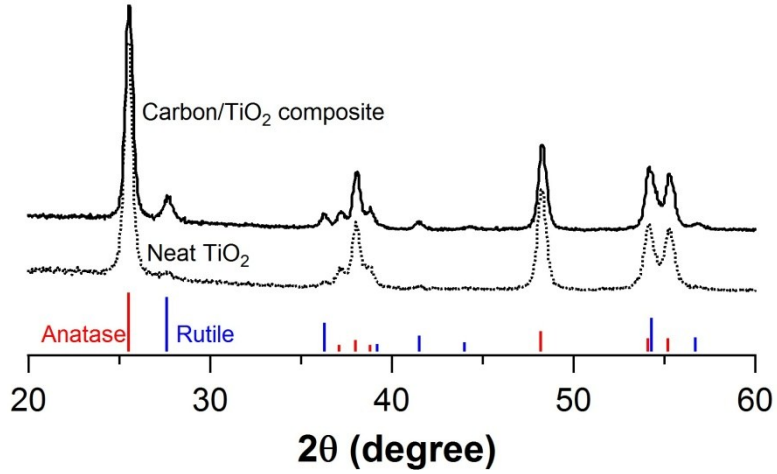

	Anatase	Rutile
Neat TiO_2	98.3 %	1.7 %
Carbon/TiO_2 composite	89.6 %	10.4 %

Figure S5. XRD profiles for the neat TiO_2 and carbon/TiO_2 composite produced by carbonization of PHBMA/PFA polymer blend with TiO_2 and the standard spectrum of anatase TiO_2 (JCPDS 84−1286, red lines) and rutile TiO2 (JCPDS 75-1753, blue lines).

The XRD in Figure S5 illustrates that the carbonized composite still contains anatase TiO_2 nanoparticles with strong diffraction peaks at ~26° and ~48°. These peaks are in good agreement with the standard spectrum for anatase (JCPDS no.: 84−1286). Although the content of rutile TiO_2 increases from 1.7 % to 10.4 % after carbonization of PFA/PHEMA/TiO_2 composite, over 91 % of anatase-TiO_2 remains without transformation. The Rutile TiO_2 has strong diffraction peaks at ~28°, ~36° and ~54° (JCPDS no.: 76-1940).

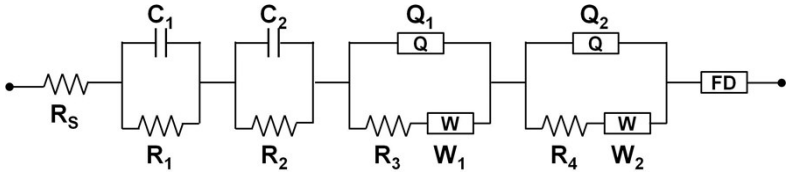

	R_S (Ω)	R_1 (Ω)	R_2 (Ω)	R_3 (Ω)	R_4 (Ω)	C_1 (F)	C_2 (F)	Q_1 ($S \cdot s^n$)	Q_2 ($S \cdot s^n$)	W_1 ($S \cdot s^{1/2}$)	W_2 ($S \cdot s^{1/2}$)
PHEMA 20K	3 ± 0.5	174 ± 44	266 ± 40	86 ± 5	21 ± 3	(1.8±1.8) × 10^{-1}	(9.4±2.4) × 10^{-6}	(3.0±2.9) × 10^{-4}	(2.1±2.1) × 10^{-3}	(3.8±0.5) × 10^{-2}	(2.1±2.1) × 10^{-4}
PHEMA 300K	15 ± 0.2	339 ± 9	439 ± 16	465 ± 8	12 ± 3	(3.2±0.3) × 10^{-5}	(8.8±0.4) × 10^{-6}	(2.7±0.1) × 10^{-4}	(1.8±0.1) × 10^{-2}	(2.6±0.8) × 10^{5}	(2.7±1.7) × 10^{-12}
PHEMA 1000K	17 ± 7	336 ± 50	202 ± 30	394 ± 105	61 ± 27	(2.7±1.3) × 10^{-5}	(3.2±3.2) × 10^{-6}	(2.9±2.0) × 10^{-3}	(1.9±0.9) × 10^{-4}	(2.9±0.8) × 10^{-2}	(5.0±3.8) × 10^{4}
FA 0.2 g	10 ± 6	190 ± 49	229 ± 30	0.1 ± 0.01	21 ± 9	(6.4±0.6) × 10^{-4}	(2.8±1.2) × 10^{-5}	(5.2±4.0) × 10^{-12}	(3.0±2.0) × 10^{-3}	(1.8±0.2) × 10^{-2}	(3.3±3.1) × 10^{-2}
FA 0.3 g	3 ± 0.5	174 ± 44	266 ± 40	86 ± 5	21 ± 3	(1.8±1.8) × 10^{-1}	(9.4±2.4) × 10^{-6}	(3.0±2.9) × 10^{-4}	(2.1±2.1) × 10^{-3}	(3.8±0.5) × 10^{-2}	(2.1±2.1) × 10^{-4}
FA 0.5 g	10 ± 0.2	180 ± 3	205 ± 7	134 ± 7	573 ± 16	(2.4±0.3) × 10^{-5}	(7.5±0.3) × 10^{-6}	(3.9±0.4) × 10^{-4}	(4.6±0.3) × 10^{-3}	(2.3±0.2) × 10^{-2}	(9.8±1.5) × 10^{4}
FA 0.7 g	9 ± 3	190 ± 20	27 ± 23	154 ± 36	2 ± 0.2	(8.5±0.4) × 10^{-6}	(1.5±0.2) × 10^{-5}	(4.7±1.3) × 10^{-4}	(6.1±1.0) × 10^{-3}	(5.4±4.6) × 10^{4}	(2.1±2.1) × 10^{9}

Figure S6. Equivalent circuit to fit the EIS data of porous carbon/TiO_2 composite electrodes and numerical values of the equivalent circuit components obtained for the impedance data.

In Figure S6, R_S indicates the bulk resistance of electrolyte, separator, and electrode. These composite anode electrodes consist of carbon and TiO_2 particles. Therefore, it leads to two different SEIs (C_1//R_1 and C_2//R_2) on carbon and TiO_2 surfaces. The interfacial charge transfer, Na ion diffusion impedance, and double layer capacitance for carbon and TiO_2 are also considered individually, and thus they are presented by a combination of Q_1//(R_3-W_1) and Q_2//(R_4-W_2) circuits in series. FD is the finite length diffusion impedance.

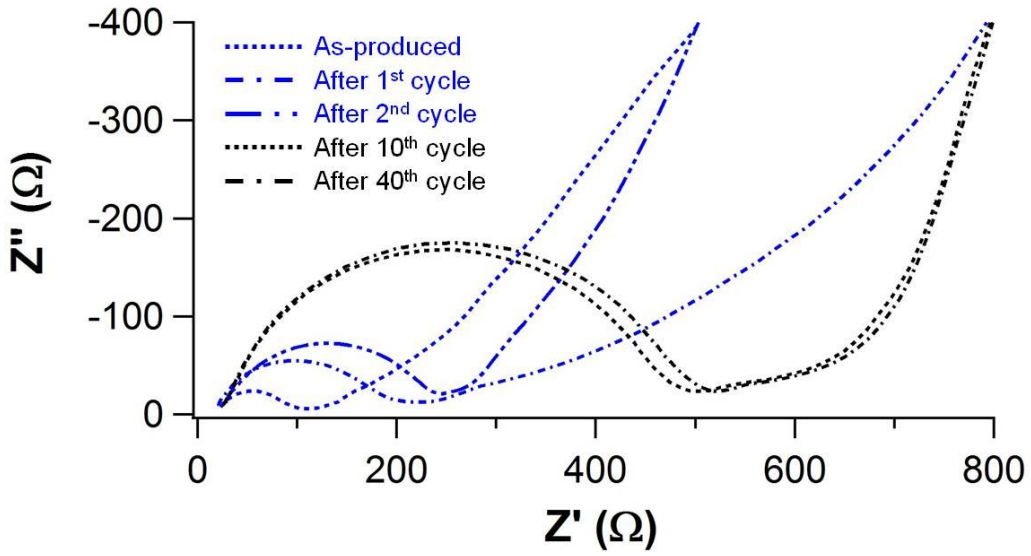

Figure S7. Nyquist plot from EIS data associated with cycling of carbon/TiO_2 composites from 20K of PHEMA and 0.3 g of FA. The impedance changes significantly in the first 10 charge-discharge cycles.

Cyclic voltammetry was carried out by cycling a carbon/TiO_2 composite from 20K of PHEMA for 40 cycles between 0.01 and 2.0 V at a scan rate of 0.01 mV/s. Figure S8 shows the corresponding CV response, with oxidation currents shown as positive and reduction currents shown as negative.

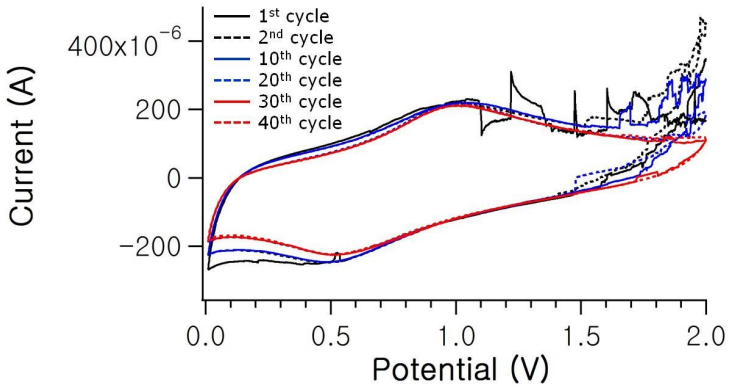

Figure S8. Cyclic voltammetry of the carbon/TiO_2 composite from 20K of PHEMA and 0.3 g of FA at a scan rate of 0.01 mV/s with sodium metal as both counter and reference electrodes.

The distribution of pore size of carbon/TiO_2 composites is shown in Figure S9. The small size pores (<6 nm) are more formed in carbon/TiO_2 composites with increasing the molecular weight of PHEMA in the precursor from 20 kg/mol to 1000 kg/mol. This indicates that the morphology of porous carbon/TiO_2 composites pyrolyzed from PHEMA/FA/TiO_2 can be controlled by the molecular weight of PHEMA used as a thermal decomposition matrix.

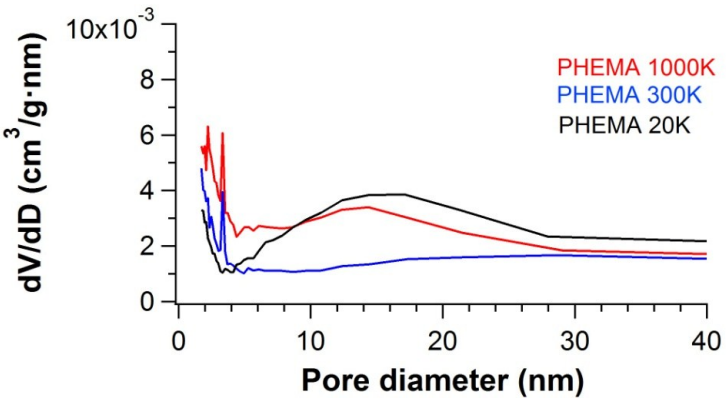

Figure S9. Pore size distribution of carbon/TiO_2 composites fabricated with 20K, 300K, and 1000K PHEMA using 0.35 g PHEMA/0.3 g FA/0.3 g TiO_2 for the precursor.

Figure S10 shows the XPS spectra of the neat and 40 charge-discharge cycled carbon/TiO_2 composite anodes fabricated with 20K, 300K, and 1000K PHEMA using 0.35 g PHEMA/0.3 g FA/0.3g TiO_2 for the precursor. All the cycled samples show that the Na1s peak appears and the intensity of O1s peak increase compared to the neat anodes. It indicates that the sodium- included inorganic compounds and oxygen-rich substances form on the surface of anodes as the SEI layer.

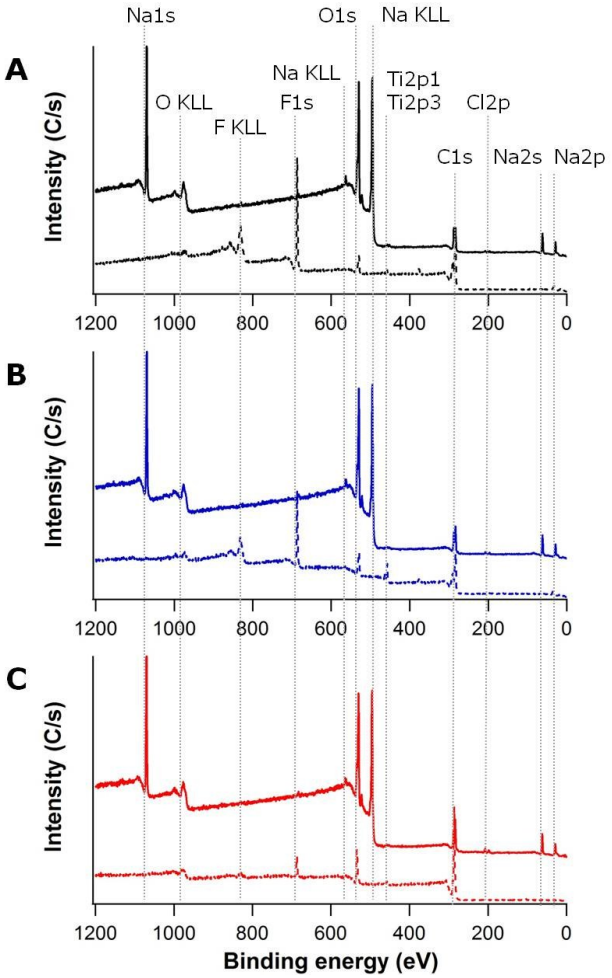

Figure S10. XPS spectra of neat (dash line) and 40 charge-discharge cycled (solid line) carbon/TiO_2 composite anodes fabricated with (A) 20K, (B) 300K, and (C) 1000K PHEMA using 0.35 g PHEMA/0.3 g FA/0.3g TiO_2 for the precursor.

Figure S11 illustrates the morphology of the porous carbon/TiO_2 composite fabricated using 0.35 g PHEMA (20K)/FA/0.3 g TiO_2 as a function of molecular weight of FA (0.2, 0.3, 0.5 and 0.7 g). The pores of the carbon/TiO_2 composite are significantly larger for the composite produced using 0.3 g (Figure S11B) than the carbon/TiO_2 composites from 0.5 g (Figure S11C) and 0.7 g FA (Figure S11D). Figure S11A illustrates the carbon/TiO_2 composite fabricated with 0.2 g FA, which has larger apertures and exposes more TiO_2 particles than other composites because it has small carbon content.

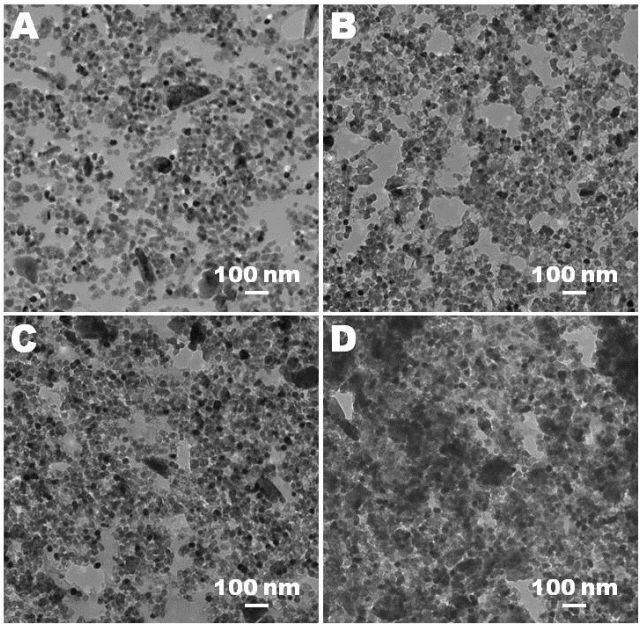

Figure S11. TEM micrographs of porous carbon/TiO_2 composites fabricated with 0.35 g PHEMA (20K)/0.3 g TiO_2/FA of (A) 0.2, (B) 0.3, (C) 0.5, and (D) 0.7 g for the precursor.

The TGA under air atmosphere is hired to confirm the carbon content of the porous carbon/TiO_2 composite fabricated using 0.35 g PHEMA (20K)/FA/0.3 g TiO_2 as a function of amount of FA (0.2, 0.3, 0.5 and 0.7 g). The TGA curves are shown in Figure S12, and the values are 12, 15, 16, and 18 wt% for the composites using 0.2, 0.3, 0.5, and 0.7 g FA, respectively.

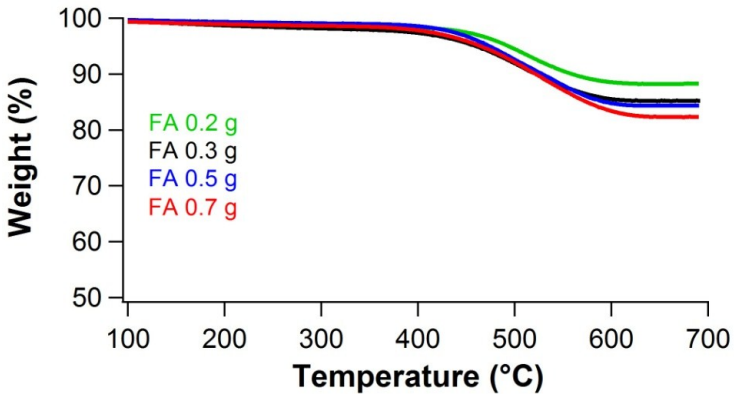

Figure S12. TGA curves of carbon/TiO_2 composites with different amount of FA to determine the carbon content by oxidation in air.

The distribution of pore size of carbon/TiO_2 composites is shown in Figure S13. The small size pores (<6 nm) are more formed in carbon/TiO_2 composites with increasing the amount of FA in the precursor from 0.3 g to 0.7 g. The carbon/TiO_2 composite fabricated with 0.2 g FA has the largest apertures, but also exposes a significant fraction of the TiO_2 nanoparticles. This indicates that the morphology of porous carbon/TiO_2 composites pyrolyzed from PHEMA/FA/TiO_2 can be controlled by the amount of FA used in the synthesis.

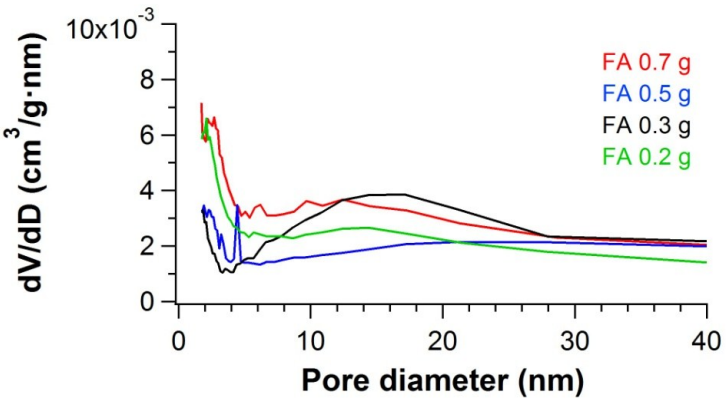

Figure S13. Pore size distribution of carbon/TiO_2 composites fabricated with 0.35 g PHEMA (20K)/0.3 g TiO_2/different amount of FA for the precursor.

Figure S14 shows the XPS spectra of the neat and 30 charge-discharge cycled carbon/TiO_2 composite anodes fabricated with different carbon contents. It indicates that the sodium- included inorganic compounds and oxygen-rich substances form on the surface of anodes as the SEI layer.

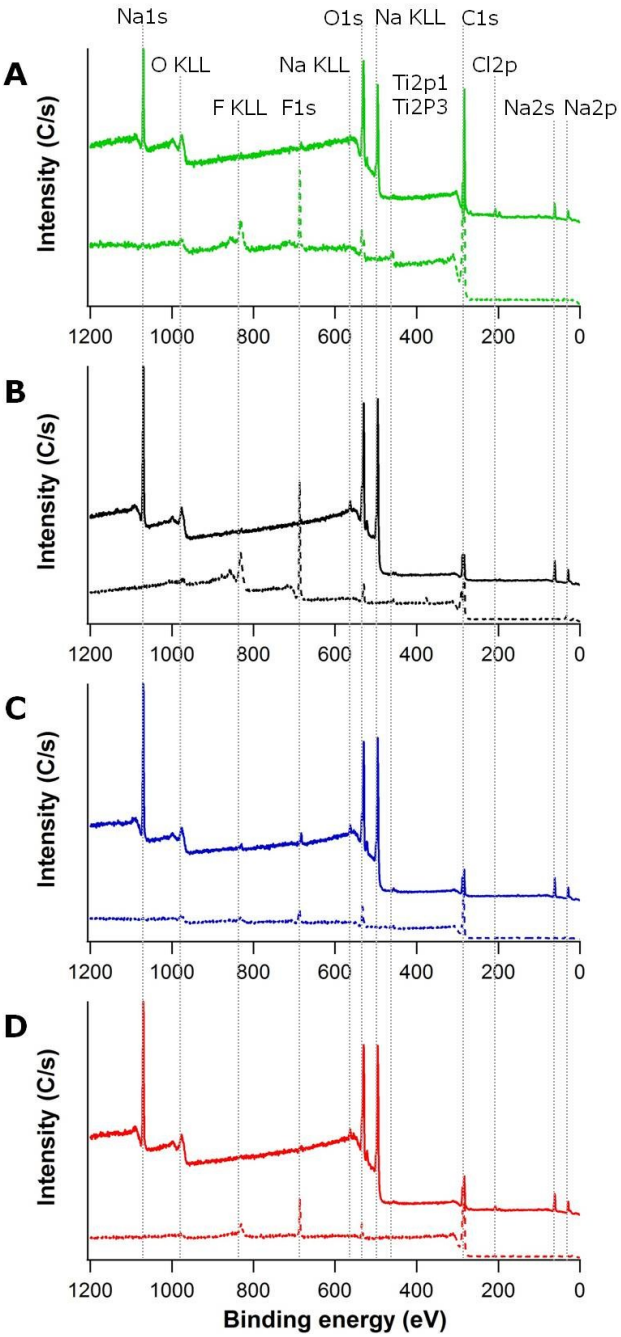

Figure S14. XPS spectra of the neat (dash line) and 30 charge-discharge cycled (solid line) composite anodes fabricated with different carbon contents of carbon/TiO_2 composite: (A) 12 wt%, (B) 15 wt%, (C) 16 wt%, and (D) 18 wt%.